

Adsorption Characteristics of Magnesium-Modified Bentonite Clay with Respect to Acid Blue 129 in Aqueous Media

Sajjad Hussain^{1*}, Zia Ullah², Saima Gul³, Rozina Khattak³,
Nida Kazmi², Fozia Rehman⁴, Sabir Khan⁵, Khalid Ahmad⁵,
Mohammad Imad¹, Adnan Khan²

¹Faculty of Materials and Chemical Engineering, GIK Institute of Engineering Sciences and Technology Topi, 23460, KPK, Pakistan

²Institute of Chemical Sciences, University of Peshawar, 25120, KPK, Pakistan

³Department of Biochemistry, Shaheed Benazir Bhutto Women's University, Peshawar, KPK, Pakistan

⁴Interdisciplinary Research Center In Biomedical Materials (IRCBM), COMSAT Institute, Lahore, Pakistan

⁵Institute of Chemistry, State University of Campinas, CEP 13083-970 Campinas, SP, Brazil

Received: 13 February 2016

Accepted: 20 March 2016

Abstract

Locally available bentonite clay has been modified by magnesium and used to eliminate acid blue 129 from aqueous solutions. The adsorption was studied under different experimental conditions such as dye concentrations, temperature, and shaking time. The adsorption of the dye increased with time and followed the pseudo-first-order kinetic with rate constant " k " 0.126 min^{-1} at 283 K. Thermodynamic parameters such as ΔH° , ΔS° , and ΔG° were calculated from the slope and intercept of the linear plots of $\ln K$ against $1/T$. Analysis of adsorption results obtained at temperatures of 283, 293, 303, and 313 K showed that the adsorption pattern on bentonite seems to follow Langmuir and Freundlich. The increase in temperature reduces adsorption capacity by magnesium-modified bentonite due to the enhancement of the desorption step in the mechanism. The activation energy of the adsorption process was found to be 3.55 kJ mol^{-1} . The Mg-bentonite showed better adsorption than Ba and Al-bentonite. Our study reveals that abundantly available local clay may be used to eliminate dyes from aqueous solutions.

Keywords: acid blue, clay, adsorption, isotherms, kinetics, bentonite

Introduction

Dyes and pigments are used in many industries to color their products. The effluents discharged by the dye industry are highly colored and are a major cause of environmental pollution [1]. Dyes are resistant to light, oxidizing agents, and heat due to their chemical nature, and are also biologically non-degradable and cannot be easily decolorized once released into an aquatic environment [2-3]. The strong colors imparted by the dyes cause aesthetic and ecological problems to aquatic ecosystems [4-6].

In particular, the presence of dye-containing effluents into a water environment may be carcinogenic and mutagenic and may cause intense damage to human beings, including the reproductive system, liver, brain, central nervous system, and dysfunction of kidneys [7].

Wastewater treatment methods such as coagulation [8], ozonation and filtration [9], oxidation, [10], sedimentation, flotation, [11] reverse osmosis, nano filtration [12], electrochemical oxidation [13], and photo-electrochemical oxidation [14] are used to treat water-containing dyes from the textile industries, but all these processes must be considered for economic reasons. Adsorption has proven to be very efficient at removing dye pollutants from effluent [4, 15-16]. The interaction of wastewater molecules to the surface of the adsorbent may be expressed in terms of both adsorptive characteristics and physical properties of the adsorbent [17]. The acid dyes can be successfully removed with activated carbon [18] and with sepiolite [19], and these processes have been carried out by many researchers. It has been found that due to high adsorption capacity, high surface area, micro porous structure, and the high degree of surface reactivity of activated carbon, it is widely used, but there are some problems with its use such as being expensive in nature due to the operational costs of activated carbon. The researchers are looking for cheaper, easily available materials for dye adsorption [20-21]. Various types of clay sepiolite [19], zeolite [22], montmorillonite [23-24], smectite [25], and bentonite [26] may be used as alternative low-cost adsorbents for treating dye effluents. Specific surface area, high chemical and mechanical stability, and various structural and surface properties make the clays widely useful. The sorption ability of a clay is usually determined by its chemical and pore structure.

Bentonite (i.e., montmorillonite clay) is normally characterized by one aluminum (Al) octahedral sheet placed between two silicon (Si) tetrahedral sheets. The negative surface charge on the bentonite is produced due to isomorphous substitution of Al^{3+} for Si^{4+} in the tetrahedral layer and Mg^{2+} for Al^{3+} in the octahedral layer. The exchangeable cations (Ba^{2+} , Mg^{2+} , etc.) imbalance the charge at the bentonite surface and both Ba^{2+} and Mg^{2+} are heavily hydrated in the presence of water, making the Bentonite's surface hydrophilic in nature [27].

The specific surface area of the clay samples can be greatly increased by acid activation and therefore acid-activated clays can be used effectively as decolorizing agents for various industries [28]. The surface properties

of bentonite clay can also be greatly modified with simple ion-exchange reactions by using a cations exchanger like H^+ , Mg^{2+} , and Ba^{2+} . This is favored by van der Waals interaction between the cations and clay. These cations occupy the exchange sites of bentonite clay and hence the surface area is increased. This kind of cationic bentonite has been used extensively for a wide variety of environmental applications [29]. This work aims to investigate the effectiveness of magnesium-modified bentonite toward acid blue 129 removal. Adsorption isotherm techniques are used to examine the adsorption capacities of dye. The rate constants and activation energy of adsorption process were used to calculate kinetics and thermodynamic parameters. Langmuir and Freundlich equations are applied to the experimental data in order to determine the isotherm that gives the best correlation to the experimental data.

Material and Methods

Material Preparation and Chemicals

The bentonite clay sample was collected from Nowshera city KPK, Pakistan. The Clay sample was ground into powder manually and the wet sedimentation process was used to get refined particles of the clay. Initially 50 g of raw bentonite was refluxed with 1 molar of hydrochloric acid for two hours in a round-bottomed flask at 80°C. The slurry was air cooled and washed with doubly distilled water and then the clay was dried in an oven at 120°C. After complete drying, 50 g of clay was added to 1 molar of MgCl_2 solution and stirred for 24 hours on a magnetic stirrer. It was then air cooled, dried, and washed with doubly distilled water four times to eliminate free salts, and finally dried in an oven at 150°C. Acid Blue 129 from Aldrich Chemicals Pakistan (and used as received) was employed as a pollutant. All other chemicals – HCl, NaOH, and MgCl_2 – were obtained from Aldrich.

Characterization of Samples

The textural structure of the clay sample was measured by N_2 adsorption at NOVA 2200e Quanta Chrome, USA. All samples were degassed at 373 K for 2 h, prior to the adsorption experiments. The BET surface area and pore volume were obtained by applying the Langmuir method. Microstructure and surface morphology of the adsorbent samples were characterized by a JEOL 5910 field emission scanning electron microscope (SEM) with an accelerating voltage 15.0 kV at 1,500x magnification.

Adsorption Tests

The adsorption tests were conducted by batch experiments. In each assay, 0.1 g of modified magnesium clay and 30 ml of solution with 4×10^{-5} mol L^{-1} concentration of AB129 (Fig. 1.) filled a bottle and

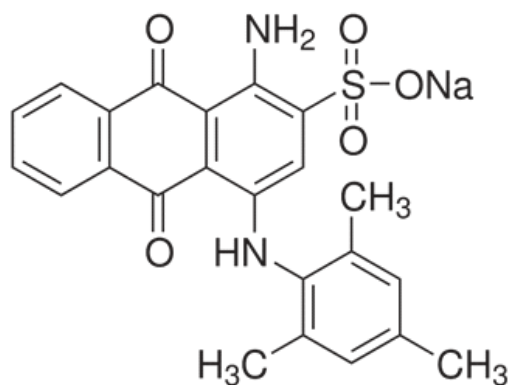


Fig. 1. Chemical structure of dye AB129.

were put in a shaker at 120 rpm. The samples were taken out, filtered, and analyzed (using a Shimadzu UV-160 A) at λ_{\max} 629 nm, and the amount of dye adsorbed (q_e , mol g⁻¹) was calculated accordingly [30-31].

Results and Discussion

Characterization of Mag-Bentonite

The surface area was calculated using Langmuir method and revealed that Mg-, Ba-, and Al-modified clay are, respectively, 1310.03, 1010.22, and 878.77 m² g⁻¹. Figs S1, S2, and S3 of supplementary information show the SEM images of the Mg-, Ba-, and Al-bentonite clay, respectively, and it can be observed that clay constituted of hollowed spheres of different sizes and some other agglomerated unshaped fragments can also be seen in S1, but large particles can be observed in S2 and S3, which may cause a reduction in adsorption of dye molecules. Elemental analysis is presented in Figs S4, S5, and S6

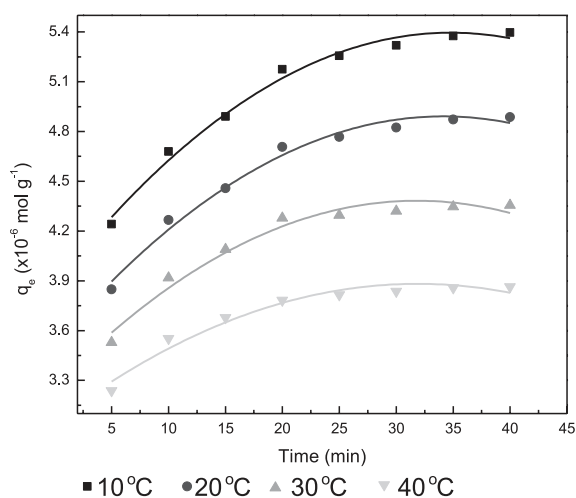


Fig. 2. Time versus amount adsorbed (q_e) plot of AB129 (pH = 3.0) adsorption by Mg-bentonite, (0.1 g/30 mL) at 10°C, 20°C, 30°C, and 40°C.

of supplementary for Mg-, Ba-, and Al-bentonite, and the presence of O₂, Si, Al, Mg, Ba, Fe, and Cl may be observed in these EDX spectra.

Batch Adsorption Studies

Effect of Contact Time

We studied the adsorption of acid blue 129 ions on Mg-bentonite clay from aqueous solution at different temperatures (Fig. 2). The results make it clear that the adsorption on Mg-bentonite clay increases with time. Furthermore, the dye uptake by activated Mg-Bentonite clay was rapid initially up to 25 minutes, followed by a continued rise up to 40 minutes, and 5.397×10^{-6} mol g⁻¹ of AB129 was adsorbed on Mg-Bentonite at 10°C. The 40 minutes were taken as equilibrium time and used for further study. The initial rapid uptake from solution was due to extra cellular bonding and the slow sorption phase likely resulted from intracellular binding.

Effect of Temperature

Fig. 3 also shows the effect of temperature on the adsorption of AB129 ions on Mg-bentonite clay. You can observe in Fig. 2 that the amount of adsorption decreases from 5.400×10^{-6} mol g⁻¹ to 3.864×10^{-6} mol g⁻¹ with the rise in temperature from 10 to 40°C, which means that AB129 ion adsorption from aqueous solution is more practical at low temperatures. The data in Table 1 also showed that the adsorption capacity of Mg-bentonite clay decreases with the increase in temperature. This is due to the dye molecules escaping from solid phase to bulk phase when there is an increase in temperature of the solution.

Effect of Initial Dyes Concentration

The influence of the initial concentration of AB129 in the solutions on the rate of adsorption onto Mg-bentonite was investigated at various concentrations at pH 3.

It is clear from Fig. 3 that the adsorption of AB129 increases from 15.15 to 67.92×10^{-5} mol g⁻¹ as the concentration increases from 1.0 to 6.0×10^{-7} mol L⁻¹ in 40 min of treatment at constant pH. This is due to the greater availability of AB129 ions to the active sites of the activated clay. It is clear from Fig. 3 that at low concentrations most of the AB129 ions are adsorbed. At higher concentration there is no significant effect on the AB129 ions due to the saturation of the surface. This indicates that the initial dye concentration plays an important role in the adsorption capacities of AB129 onto Mg-bentonite clay.

Kinetics of Adsorption

In order to investigate the kinetics of adsorption of acid blue 129 on Mg-bentonite clay, the Lagergren equation (Eq. 1) was found to apply to the adsorption data:

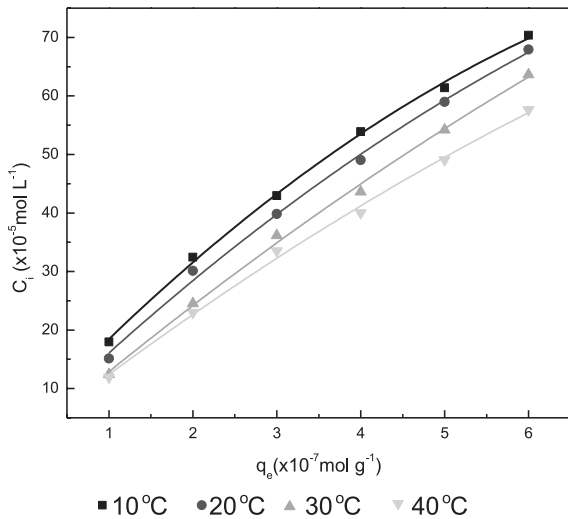


Fig. 3. Effect of initial acid blue 129 concentration for the adsorption by Mg-bentonite clay (0.1 g/30 mL) at pH 3.0 and 10°C, 20°C, 30°C, and 40°C.

$$\log(q_e - q_t) = \log q_e - \frac{k_1 t}{2.303} \quad (1)$$

...where q_e and q_t are the amount of AB129 (mol g^{-1}) adsorbed at equilibrium and at time t , respectively, and k_1 is overall rate constant. Straight lines were obtained by plotting $\log(q_e - q_t)$ against t , as shown in Fig. 4. These straight lines indicate that the adsorption process follows first-order kinetics. The values of rate constant k were calculated from the slopes of straight lines of Fig. 4 and are given in Table 1, which increases with increases in temperature. The activation energy E_a for adsorption was calculated using the Arrhenius equation and was found to be 3.550 $kJ\ mol^{-1}$.

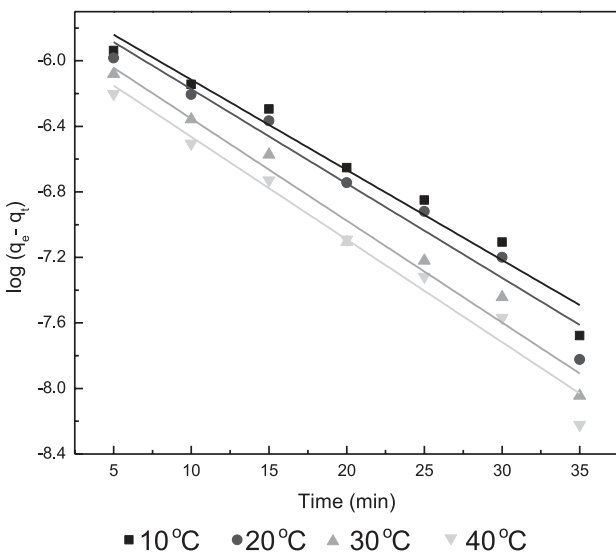


Fig. 4. Time versus $\log(q_e - q_t)$ plot of AB129 (pH = 3.0) adsorption by Mg-bentonite (0.1 g/30 mL) at 10°C, 20°C, 30°C, and 40°C.

Table 1. Rate constant and activation energy parameters for the adsorption of AB129 on Mg-bentonite at different temperatures.

T ($^{\circ}C$)	q_e (mol g^{-1})	k_1 (min $^{-1}$)	R^2	$1/T$ ($\times 10^{-3}\ K^{-1}$)	E_a (kJ mol^{-1})
10	5.397	0.126	0.9961	3.53	3.550
20	4.887	0.132	0.9615	3.41	
30	4.356	0.143	0.9734	3.3	
40	3.864	0.144	0.9743	3.19	

Adsorption Equilibrium

The equilibrium adsorption study of AB129 on Mg-bentonite clay was evaluated at 10°C, 20°C, 30°C, and 40°C. Two isotherm equations were applied since the adsorption isotherm plays a vital role in studying the nature of the adsorption system. The data of this study is evaluated by applying the Langmuir and Freundlich isotherms. The linear form of Langmuir (Eq. 2) was applied to the adsorption data:

$$\frac{C_e}{q_e} = \frac{1}{K_1 X_m} + \frac{C_e}{X_m} \quad (2)$$

...where C_e is the equilibrium concentration (M), q_e is the amount (mol g^{-1}) of AB129 adsorbed, and X_m and K_1 are Langmuir constants that represent adsorption capacity (mol g^{-1}) and energy of adsorption (mol g^{-1}), respectively. Fig. 5 C_e/q_e against C_e indicate the applicability of the Langmuir adsorption isotherm, consequently the formation of the monolayer surface of the adsorbate on the surface of the adsorbent. Langmuir constant X_m (adsorption capacity) and K_1 (binding energy constant of adsorption or energy of

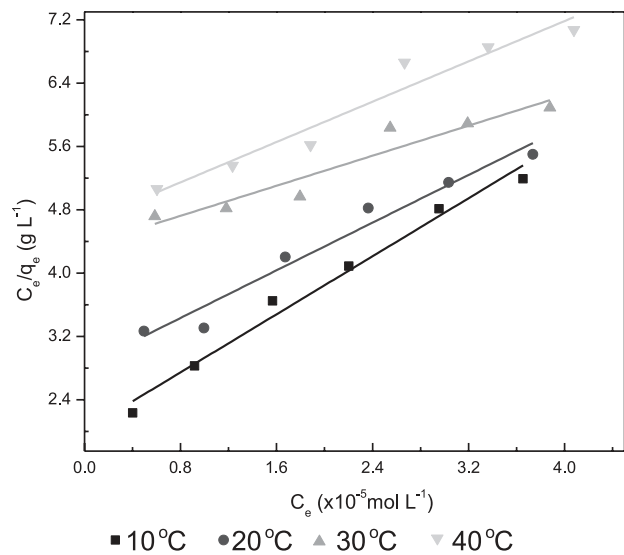


Fig. 5. Langmuir adsorption isotherms for adsorption of acid blue 129 over Mg-bentonite clay (0.1 g/30 mL) at pH 3.0 and 10°C, 20°C, 30°C, and 40°C.

Table 2. Isotherm parameters for the adsorption of AB129 on Mg-bentonite at different temperatures.

T(°C)	Langmuir constant				Freundlich constant		
	$Xm_j(x10^{-5} \text{ mol g}^{-1})$	$K_j(x10^4 \text{ mol L}^{-1})$	R_L	R^2	$1/n \text{ (g L}^{-1}\text{)}$	$K(x\mu\text{mol g}^{-1})$	R^2
10	1.215	4.2092	0.70	0.9913	0.411	1.603	0.9946
20	1.489	2.3405	0.81	0.9592	0.436	1.393	0.9838
30	2.350	0.9595	0.51	0.9019	0.509	1.030	0.9778
40	1.653	1.3504	0.88	0.9404	0.479	1.018	0.9925

adsorption) were calculated from the slopes and intercepts of plots of C_e/q_e against C_e , respectively, and are given in Table 2.

The Langmuir isotherm also reveals that the adsorption of AB129 dye is feasible onto Mg-bentonite based on separation factor (dimensionless constant) R_L which is given by the following equation:

$$R_L = 1 / (1 + K_a C_0) \tag{3}$$

Adsorption of any contaminant is regarded as favorable if R_L values follow $0 < R_L < 1$, whereas $R_L > 1$ (unfavorable), $R_L = 1$ (linear), and $R_L = 0$ (irreversible). An R_L value less than 1 shows that adsorption of AB129 is favorable onto Mg-bentonite (Fig. 5).

The Freundlich isotherm is an empirical equation employed to describe the heterogeneous system. The linear form of Freundlich isotherm (Eq. 4) was also applied to the adsorption data of AB129 ions as given in Table 2.

$$\ln \frac{x}{m} = \ln K + \frac{1}{n} \ln C_e \tag{4}$$

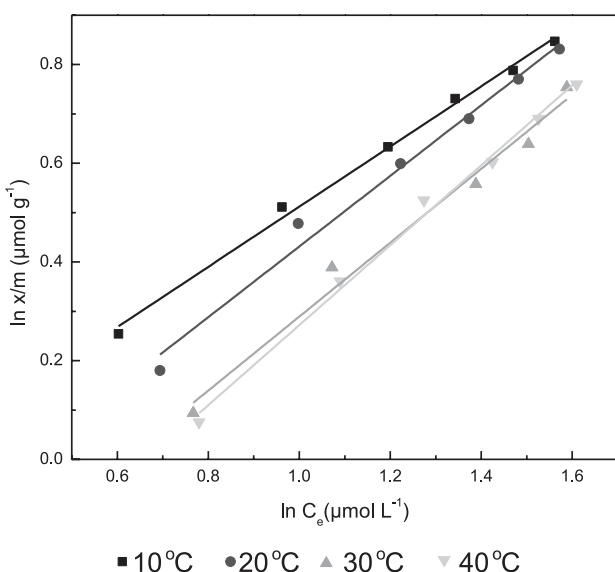


Fig. 6. Freundlich adsorption isotherms for adsorption of acid blue 129 over Mg-bentonite (0.1 g/30 mL) at pH 3.0 and 10°C, 20°C, 30°C, and 40°C.

...where $K \text{ (mol g}^{-1}\text{)}$ and $1/n \text{ (g L}^{-1}\text{)}$ are Freundlich constants, indicating adsorption capacity and adsorption intensity, respectively. Fig. 6 shows the Freundlich profile and the values are demonstrated in Table 2. This isotherm fits better than the Langmuir isotherm ($R_2 > 0.994$) to the adsorption data. As the values of $1/n$ increase with increasing temperature, it indicates favorable adsorption at lower temperatures. The values of $1/n$ indicate the formation of a relatively stronger bond between adsorbate and adsorbent as temperature decreases. When the values of K and $1/n$ (Freundlich constant) were compared at all the temperatures under study, the results show that higher values of $1/n$ and lower values of K were obtained at higher temperatures.

Adsorption Thermodynamic

The influence of temperature on AB129 adsorption is further explained by thermodynamic parameters. Various thermodynamic parameters such as ΔG° , ΔH° , and ΔS° of AB129 adsorption were calculated from Langmuir's binding constant K_1 by using equations 5 and 6. The values of ΔH° and ΔS° were calculated from the slope and intercept, respectively, of linear variation of $\ln K_1$ versus $1/T$ (Fig. 7) using Equation 7:

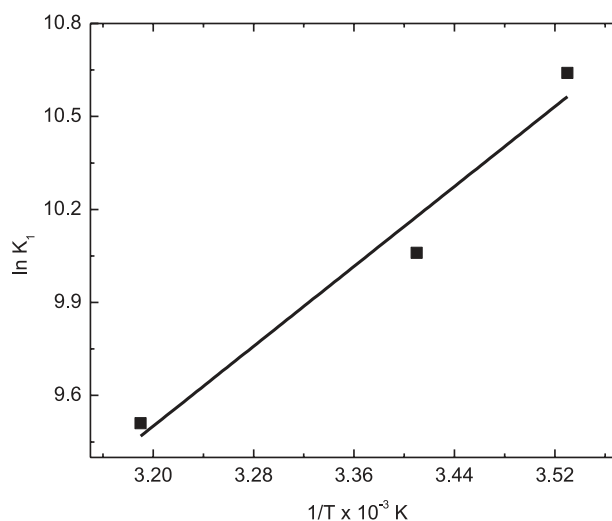


Fig. 7. Plot of $\ln K_1$ vs. $1/T$ for the adsorption of AB129 on Mg-bentonite clay.

Table 3. Thermodynamic parameters for the adsorption of AB129 on Mg-bentonite at different temperatures.

$T (^{\circ}\text{C})$	$1/T \times 10^{-3} (\text{K}^{-1})$	$\ln K_1$	$\Delta H (\text{kJ mol}^{-1})$	$\Delta S (\text{kJ mol}^{-1} \text{K}^{-1})$	$\Delta G (\text{kJ mol}^{-1})$	R^2
10	3.53	10.64	-31.83	-25.03	-25.05	0.879
20	3.41	10.06			-24.50	
30	3.30	9.168			-23.09	
40	3.19	9.510			-24.74	

$$\Delta G^{\circ} = -RT \ln K_1 \quad (5)$$

$$\ln K_1 = -\frac{\Delta H^{\circ}}{RT} + \frac{\Delta S^{\circ}}{R} \quad (6)$$

...where R is the ideal gas constant ($8.314 \text{ J mol}^{-1} \text{ K}^{-1}$) and T is the absolute Temperature in kelvin. The values of ΔS° , ΔG° , and ΔH° are given in Table 3. The negative values of ΔG° -25.05, -24.50, -23.09, and -24.74 kJ mol^{-1} at 10, 20 30, and 40°C show the spontaneous nature of the adsorption process. The values obtained for ΔG° are nearly constant, showing that there is no effect of temperature on the free energy of adsorption. The negative value ($-31.83 \text{ kJ mol}^{-1}$) of ΔH° shows that the process of adsorption is exothermic in nature. Moreover, the values of ΔH° ($> -8 \text{ kJ mol}^{-1}$) verify that AB129 adsorption is a physical process [32]. The value of ΔS° is also negative because adsorption involves more order arrangement, or in other words disorderliness decreases, resulting in a decrease in entropy.

Comparison of Adsorption Capacity of Mg-Bentonite and Ba, Al-Bentonite Clay

The bentonite clay was also treated with Al and Ba and their capacity was compared to Mg-bentonite clay at the same experimental conditions. Fig. 8 demonstrates that Mg-bentonite has better adsorption ability for the removal of AB129 from aqueous solution than Ba and Al bentonite, mainly because of its porous surface and small particle size. The SEM images in supplementary material explain

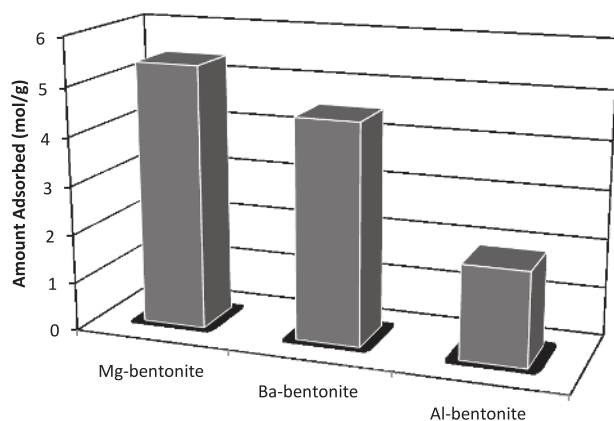


Fig. 8. Comparison of the adsorption capacity of Mg-bentonite with Ba and Al-bentonite at pH 3.

the porosity and small particle size of Mg-bentonite. Natural bentonite is not a more effective adsorbent for the removal of hydrophobic organic compounds from aqueous solution, which is due to the electrically charged and hydrophilic characteristics of the surface. However, natural bentonite may be modified to improve its capability of removing hydrophobic contaminants from water.

Conclusion

The results demonstrate that naturally occurring clay bentonite has sufficient adsorptive properties and can be used as a promising adsorbent to remove AB129 dyes from an aqueous solution after chemical activation. The adsorption process was fast and equilibrium between AB129 in the solution and on the Mg-Bentonite surface was achieved in 40 minutes. Adsorption kinetics adequately obey the pseudo first-order model ($R_2 > 0.994$). Adsorption isothermal studies reveal that the Freundlich model fits the experimental data well ($R_2 > 0.996$). The negative values of ΔG° showed that the adsorption process was spontaneous and physisorptive. These results showed that AB 129 could be successfully removed from aqueous solution using Mg-bentonite clay as a cheap adsorbent.

Acknowledgements

The authors gratefully acknowledge the cooperation of lab technicians/assistant for the characterization of clay samples at the Centralized Recourse Laboratory (CRL) University of Peshawar, Pakistan.

References

- KADIRVELU K., KAVIPRIYA M., KARTHIKA C., RADHIKA M., VENNILAMANI N., PATTABHI S. Utilization of various agricultural wastes for activated carbon preparation and application for the removal of dyes and metal ions from aqueous solutions. *Bioresour. Technol.* **87**, 129, 2003.
- WON S.W., CHOI S.B., YUN Y-S. On the reason why acid treatment of biomass enhances the biosorption capacity of cationic pollutants. *Korean J. Chem. Eng.* **31**, 68, 2013.
- ROBINSON T., CHANDRAN B., NIGAM P. Effect of pretreatments of three waste residues, wheat straw, corncobs and barley husks on dye adsorption. *Bioresour. Technol.* **85**, 119, 2002.

4. MITTAL A., THAKUR V., MITTAL J., VARDHAN H. Process development for the removal of hazardous anionic azo dye Congo red from wastewater by using hen feather as potential adsorbent. *Desalin. Water Treat.* **52**, 227, **2014**.
5. ZHANG J., CHEN S., ZHANG Y., QUAN X., ZHAO H., ZHANG Y. Reduction of acute toxicity and genotoxicity of dye effluent using Fenton-coagulation process. *J. Hazard. Mater.* **274**, 198, **2014**.
6. DE LUNA L.A.V., DA SILVA T.H.G., NOGUEIRA R.F.P., KUMMROW F., UMBUZEIRO G.A. Aquatic toxicity of dyes before and after photo-Fenton treatment. *J. Hazard. Mater.* **276**, 332, **2014**.
7. ALVES DE LIMA R.O., BAZO A.P., SALVADORI D.M.F., RECH C.M., DE PALMA OLIVEIRA D., DE ARAGÃO UMBUZEIRO G. Mutagenic and carcinogenic potential of a textile azo dye processing plant effluent that impacts a drinking water source. *Mutat. Res. - Genet. Toxicol. Environ. Mutagen.* **626**, 53, **2007**.
8. VERMA A.K., DASH R.R., BHUNIA P. A review on chemical coagulation/flocculation technologies for removal of colour from textile wastewaters. *J. Environ. Manage.* Jan **93**, 154, **2012**.
9. FERELLA F., DE MICHELIS I., ZERBINI C., VEGLIÒ F. Advanced treatment of industrial wastewater by membrane filtration and ozonization. *Desalination.* **313**, 1, **2013**.
10. ASGHAR A., ABDUL RAMAN A.A., WAN DAUD W.M.A. Advanced oxidation processes for in-situ production of hydrogen peroxide/hydroxyl radical for textile wastewater treatment: a review. *J. Clean. Prod.* **87**, 826, **2015**.
11. ZODI S., MERZOUK B., POTIER O., LAPICQUE F., LECLERC J.P. Direct red 81 dye removal by a continuous flow electrocoagulation/flotation reactor. *Sep. Purif. Technol.* **108**, 215, **2013**.
12. KURT E., KOSEOGLU-IMER D.Y., DIZGEN, CHELLAM S., KOYUNCU I. Pilot-scale evaluation of nanofiltration and reverse osmosis for process reuse of segregated textile dyewash wastewater. *Desalination.* **302**, 24, **2012**.
13. GOMES L., MIWA DOUGLAS W., MALPASS G.R.P., MOTHEO A.J. Electrochemical Degradation of the Dye Reactive Orange 16 using Electrochemical Flow-Cell. *J. Brazilian Chem. Soc.* **1**, **2011**.
14. CATANHO M., MALPASS G.R.P., MOTHEO A.J. Photoelectrochemical treatment of the dye reactive red 198 using DSA® electrodes. *Appl. Catal. B Environ.* Feb., **62**, 193, **2006**.
15. MITTAL J., THAKUR V., MITTAL A. Batch removal of hazardous azo dye Bismark Brown R using waste material hen feather. *Ecol. Eng. Nov.* **60**, 249, **2013**.
16. HUSSAIN S., GUL S., KHAN S., UR REHMAN H. Retention studies of chromium (VI) from aqueous solution on the surface of a novel carbonaceous material. *Arab. J. Geosci. Nov;* **6**, 4547, **2012**.
17. MITTAL A., KURUP L. Column operations for the removal and recovery of a hazardous dye "acid red - 27" from aqueous solutions, using waste materials - bottom ash and de-oiled soya. *Ecol. Environ. Conserv.* **12**, 181, **2006**.
18. GUPTA V.K., MITTAL A., JAIN R., MATHUR M., SIKARWAR S. Adsorption of Safranin-T from wastewater using waste materials- activated carbon and activated rice husks. *J. Colloid Interface Sci.* **303**, 80, **2006**.
19. SANTOS S.C.R., BOAVENTURA R.A.R. Adsorption modelling of textile dyes by sepiolite. *Appl. Clay Sci.* **42**, 137, **2008**.
20. GUPTA V.K., MITTAL A., KURUP L., MITTAL J. Adsorption of a hazardous dye, erythrosine, over hen feathers. *J. Colloid Interface Sci.* **304**, 52, **2006**.
21. GHAEDI M., NASAB A.G., KHODADOUST S., SAHRAEI R., DANESHFAR A. Characterization of zinc oxide nanorods loaded on activated carbon as cheap and efficient adsorbent for removal of methylene blue. *J. Ind. Eng. Chem.* **21**, 986, **2015**.
22. ALVER E., METIN A. Anionic dye removal from aqueous solutions using modified zeolite: Adsorption kinetics and isotherm studies. *Chem. Eng. J.* **200-202**, 59, **2012**.
23. SHARMA P., BORAH D.J., DAS P., DAS M.R. Cationic and anionic dye removal from aqueous solution using montmorillonite clay: evaluation of adsorption parameters and mechanism. *Desalin. Water Treat.* **1**, **2015**.
24. BHATTACHARYYA K.G., GUPTA S. SEN, SARMA G.K. Kinetics, equilibrium isotherms and thermodynamics of adsorption of Congo red onto natural and acid-treated kaolinite and montmorillonite. *Desalin. Water Treat.* **53**, 530, **2013**.
25. CHAARI I., FEKI M., MEDHIOUB M., BOUZID J., FAKHFAKH E., JAMOSSI F. Adsorption of a textile dye "Indanthrene Blue RS (C.I. Vat Blue 4)" from aqueous solutions onto smectite-rich clayey rock. *J. Hazard. Mater.* **172**, 1623, **2009**.
26. ANIRUDHAN T.S., RAMACHANDRAN M. Adsorptive removal of basic dyes from aqueous solutions by surfactant modified bentonite clay (organoclay): Kinetic and competitive adsorption isotherm. *Process Saf. Environ. Prot.* **95**, 215, **2015**.
27. WANG C.C., JUANG L.C., HSU T.C., LEE C.K., LEE J.F., HUANG F.C. Adsorption of basic dyes onto montmorillonite. *J. Colloid Interface Sci.* **273**, 80, **2004**.
28. VELDE B. Introduction to clay minerals. Springer Netherlands; **1992**.
29. SHEN Y-H. Preparations of organobentonite using nonionic surfactants. *Chemosphere.* Aug; **44**, 989, **2001**.
30. MITTAL A., GUPTA V.K. Adsorptive removal and recovery of the azo dye Eriochrome Black T. *Toxicol. Environ. Chem.* **1813**, **2010**.
31. HUSSAIN S., GUL S., KHAN S., REHMAN H., ISHAQ M., KHAN A., JAN F.A., DIN ZU. Removal of Cr(VI) from aqueous solution using brick kiln chimney waste as adsorbent. *Desalin. Water Treat. Sep;* **1**, **2013**.
32. REHMAN M.S.U., MUNIR M., ASHFAQ M., RASHID N., NAZAR M.F., DANISH M., HAN J-I. Adsorption of Brilliant Green dye from aqueous solution onto red clay. *Chem. Eng. J. Jul;* **228**, 54, **2013**.